Applied Geochemistry 27 (2012) 1567–1578

Contents lists available at SciVerse ScienceDirect

Applied Geochemistry

journal homepage: www.elsevier.com/locate/apgeochem

Defining manganese(II) removal processes in passive coal mine drainage treatment systems through laboratory incubation experiments

Fubo Luan [a], Cara M. Santelli [b], Colleen M. Hansel [c], William D. Burgos [a,*]

[a] Department of Civil and Environmental Engineering, Pennsylvania State University, 212 Sackett Building, University Park, PA 16802, USA
[b] Smithsonian Institution, PO Box 37012, MRC 119, Washington, DC 20013, USA
[c] Harvard School of Engineering and Applied Sciences, Cambridge, MA 02138, USA

ARTICLE INFO

Article history:
Received 2 February 2012
Accepted 28 March 2012
Available online 5 April 2012
Editorial handling by R. Fuge

ABSTRACT

Oxic limestone beds are commonly used for the passive removal of Mn(II) from coal mine drainage (CMD). Aqueous Mn(II) is removed via oxidative precipitation of Mn(III/IV) oxides catalyzed by Mn(II)-oxidizing microbes and Mn oxide (MnO_x) surfaces. The relative importance of these two processes for Mn removal was examined in laboratory experiments conducted with sediments and CMD collected from eight Mn(II)-removal beds in Pennsylvania and Tennessee, USA. Sterile and non-sterile sediments were incubated in the presence/absence of air and presence/absence of fungicides to operationally define the relative contributions of Mn removal processes. Relatively fast rates of Mn removal were measured in four of the eight sediments where 63–99% of Mn removal was due to biological oxidation. In contrast, in the four sediments with slow rates of Mn(II) removal, 25–63% was due to biological oxidation. Laboratory rates of Mn(II) removal were correlated ($R^2 = 0.62$) to bacterial biomass concentration (measured by phospholipid fatty acids (PLFA)). Furthermore, laboratory rates of Mn(II) removal were correlated ($R^2 = 0.87$) to field-scale performance of the Mn(II)-removal beds. A practical recommendation from this study is to include MnO_x-coated limestone (and associated biomass) from an operating bed as "seed" material when constructing new Mn(II)-removal beds.

© 2012 Elsevier Ltd. All rights reserved.

1. Introduction

The presence of elevated concentrations of Mn(II) in coal mine drainage (CMD) is a significant problem for many regions in the USA and throughout the world. In Appalachia, centuries of coal mining have left thousands of abandoned mines that are discharging metal-contaminated CMD with Mn concentrations as high as 150 mg/L (Herlihy et al., 1990; Cravotta, 2008). Manganese, while not considered to be acutely toxic to humans, can be damaging to ecosystems and water distribution systems at such high concentrations. At operating coal mines, the most commonly used "active treatment" method to remove Mn(II) is to add caustic chemical to increase pH to >9 and precipitate $Mn(OH)_2$. At abandoned coal mines, the most commonly used "passive treatment" method to remove Mn(II) is biologically-active aerobic limestone beds, systems where the oxidation of soluble Mn(II) and subsequent precipitation of Mn(III/IV) oxide minerals (MnO_x) is catalyzed by abiotic and biotic processes (Cravotta and Trahan, 1999; Hallberg and Johnson, 2005; Johnson et al., 2005). To function effectively, passive Mn(II) removal beds require oxic conditions and very low influent concentrations of Fe and Al (to avoid hydraulic clogging) and are, therefore, typically located at the end of the passive treatment train. All Mn(II) removal beds in the current study met these criteria. In essence, Mn is immobilized within the treatment systems via the precipitation of sparingly soluble Mn oxides that vary in structure depending on the aqueous milieu, rate of oxidation and Mn(II) oxidation process (e.g., microbial versus abiotic). These freshly formed Mn oxides have a high reactivity and, through both co-precipitation and surface adsorption reactions, will further remove other soluble metal contaminants from the mine waters (e.g., Cu, Co, Zn) (Cravotta and Trahan, 1999; Tan et al., 2010). While no official inventory of all CMD treatment systems is maintained, several dozen passive Mn(II)-removal beds have been constructed in the Appalachian coalfields over the past 30 a (Brent Means, US Office of Surface Mining Reclamation and Enforcement, pers. comm.). To date, the overall success of Mn removal in passive treatment systems is widely variable due to a poor understanding of the mechanisms that govern Mn(II) oxidation at near-neutral pH in these systems.

The abiotic oxidation of Mn(II), with O_2 serving as the terminal electron acceptor, is kinetically inhibited below pH 9 (Von Langen et al., 1997). Some active treatment systems will add both caustic chemicals (to raise pH > 9) and oxidants (e.g., ozone) such that Mn(II) can be removed either as $Mn(OH)_2(s)$ or $MnO_x(s)$. However, a number of biotic and abiotic processes can catalyze Mn(II) oxidation at near-neutral pH within the environment. Microorganisms accelerate Mn(II) oxidation rates up to several orders of magnitude

* Corresponding author. Tel.: +1 814 863 0578; fax: +1 814 863 7304.
E-mail address: wdb3@psu.edu (W.D. Burgos).

0883-2927/$ - see front matter © 2012 Elsevier Ltd. All rights reserved.
http://dx.doi.org/10.1016/j.apgeochem.2012.03.010

faster than homogeneous Mn(II) oxidation by O_2, thus it is believed that the precipitation of Mn(III/IV) oxide minerals in the environment is largely driven by microbiological activity (Nealson et al., 1988; Tebo et al., 2004). More recently, however, it has been demonstrated that mineral surfaces and reactive oxygen species can oxidize Mn(II) at rates equivalent or greater than those by microorganisms (Madden and Hochella, 2005; Hansard et al., 2011; Learman et al., 2011), thus calling into question the primary Mn(II) oxidation processes *in situ*. Environmental Mn(II) oxidation is likely a result of a number of juxtaposed abiotic and biotic oxidation and adsorption reactions.

Identifying the primary Mn(II) oxidation processes in a complex, field setting is challenging. Numerous studies, however, have reported subtle differences in MnO_x-mineral structures resulting from abiotic vs. biotic processes, biogenic Mn oxides generally tend to be smaller and more reactive than synthetic analogs (Bargar et al., 2005). The primary products of microbially-catalyzed Mn(II) oxidation are nanoparticulate mineral phases with a high degree of site vacancies (Bargar et al., 2005; Webb et al., 2005a; Hansard et al., 2011; Learman et al., 2011; Santelli et al., 2011) that resemble a poorly-ordered birnessite with hexagonal symmetry. These highly reactive minerals promote autocatalytic oxidation of Mn(II) at the Mn oxide surface (Learman et al., 2011) and precipitate additional MnO_x abiotically. This high surface reactivity also results in substantial Mn(II) adsorption, which will induce the reductive transformation of the Mn oxides (e.g., $MnO_2 + Mn^{2+} \rightarrow 2MnOOH$) to more thermodynamically stable oxides over short time periods (Bargar et al., 2005; Webb et al., 2005b; Elzinga, 2011; Learman et al., 2011).

Several different species of prokaryotic bacteria and eukaryotic fungi can promote the oxidation of Mn(II). Manganese(II)-oxidizing bacteria are ubiquitously distributed in the environment and much research has recently been devoted to understanding the mechanisms, pathways, and products of Mn(II) oxidation by bacteria (Francis et al., 2001; Bargar et al., 2005; Webb et al., 2005a; Hansel and Francis, 2006; Ridge et al., 2007). Similarly, Basidiomycota and Ascomycota Mn(II)-oxidizing fungi have been recovered from a wide variety of ecosystems, such as agricultural soil (Pedler et al., 1996), deep sea sediments (Shao and Sun, 2007), building stone (Delatorre and Gomezalarcon, 1994), desert varnish (Krumbein and Jens, 1981; Grote and Krumbein, 1992), streambeds (Miyata et al., 2004, 2006; Takano et al., 2006), a constructed wetland (Takano et al., 2006), and CMD treatment systems (Robbins et al., 1992, 1997; Mariner et al., 2008; Santelli et al., 2010). To date, no Mn(II)-oxidizing archaea have been identified. Studies seeking to identify the oxidation mechanisms employed by Mn(II)-oxidizing bacteria and fungi generally have demonstrated that these organisms are heterotrophs that gain energy through oxidative respiration of organic C compounds: no energy appears to be gained from Mn(II) oxidation reactions for either bacteria or fungi.

The contribution of both bacteria and fungi to the remediation of Mn-contaminated waters has frequently been observed (Cravotta and Trahan, 1999; Robbins et al., 1992; Haack and Warren, 2003; Hallberg and Johnson, 2005; Johnson and Younger, 2005; Bamforth et al., 2006; Tan et al., 2010). Several different strains of Mn(II)-oxidizing bacteria have even been used in a patented bioremediation method, the "Pyrolucite Process", for treating manganiferous mine waters (Vail and Riley, 2000). A recent study by Mariner et al. (2008) identified Mn(II)-oxidizing fungi, in addition to bacteria, that successfully grew in a Mn(II)-removal bioreactor for treating mine water. To the authors' knowledge, this was the first study to document the role of fungi in these bioremediation systems. Santelli et al. (2010, 2011) discovered an abundant and diverse group of Mn(II)-oxidizing Ascomycota fungi isolated from passive Mn(II)-removal beds treating CMD in Appalachia. In general, however, the identities and growth characteristics of the Mn(II)-oxidizing community members contributing to Mn remediation remains largely unresolved.

The purpose of this research was to improve understanding of processes promoting Mn remediation and attenuation in passive Mn(II)-removal systems currently utilized for the treatment of coal mine drainage. The objectives of this research were to: (1) measure Mn removal kinetics in controlled laboratory experiments using sediments collected from eight different treatment systems; (2) determine the dominant processes responsible for Mn removal; and (3) identify the contribution of the indigenous microbial community to Mn removal.

2. Materials and methods

2.1. Site description and sampling techniques

Eight passive Mn(II)-removal beds were characterized in this study (seven in western Pennsylvania and one in eastern Tennessee). The systems were similar in that all were essentially rectangular beds filled to approximately 1 m depth with crushed limestone. The limestone beds were typically partially filled with water such that influent CMD flowed horizontally through saturated porous media. Sites were selected in consultation with personnel from the Pennsylvania Department of Environmental Protection and the US Office of Surface Mining Reclamation and Enforcement to provide a fairly broad representation of the geochemical and hydrological variety associated with these types of treatment systems (Table 1; Table S1; Supp. Fig. 1). Samples of MnO_x-rich sediments that had accumulated in each bed were collected for use in laboratory experiments designed to measure the rate of Mn(II) removal (Fig. 1). Sediments were typically collected at a relatively shallow depth into the limestone bed, near the air–water interface where MnO_x precipitation tended to be greatest. For four sites (Ace, Glady Fork, De Sale 2, De Sale 1), thick, soft, "soil-like", MnO_x-rich sediments were easily collected using sterile spatulas and whirl-paks. For the other four sites (De Sale 3, Fairview, Derry Ridge, PBS), thin, hard "crusts" that were cemented to the limestone cobbles had to be mechanically scraped off individual cobbles using sterile knives and brushes. All sediments were stored at field moisture at 4 °C in the dark.

Water samples were collected at the influent and effluent ends of each Mn(II)-removal bed to measure in-field performance. Samples were filtered (0.2 μm) in the field, chemically preserved (dependent on analyte) and stored on ice during transport. Dissolved O_2 (DO) concentrations, temperature, pH and conductivity were determined in the field using portable meters. Large volumes of influent water from each site were collected in 10 L high density polyethylene plastic containers and used for the laboratory experiments. These waters were filtered (0.2 μm) in the laboratory and stored at 4 °C.

2.2. Sediment incubation experiments

Laboratory sediment incubation experiments were conducted to determine the relative importance of adsorption versus oxidation processes on Mn(II) loss from solution and the relative importance of the microbial community on Mn removal. Experiments were conducted with a single, large quantity of sediment collected from each Mn(II)-removal bed. Sediments were homogenized and sieved at field moisture content (<2-mm sieve fraction) using sterile tools. Manganese oxide and moisture content of all the sediments were measured and used to calculate the mass of moist "live" sediments added to the reactors. All reactors were prepared with a sediment mass equivalent to 0.5 g MnO (dry mass) and 50 mL of filter-sterilized influent water (from the same site as for

Table 1
Physical characteristics of the eight Mn removal beds, and geochemical characteristics of the influent waters.

	Ace[a]	Glady Fork[b]	De Sale 3[c]	De Sale 2[c]	Fairview[d]	Derry Ridge[e]	De Sale 1[c]	PBS[f]
Flow rate (L/s)	1.73 ± 0.61	54.2 ± 21.5	0.74 ± 0.15	6.10 ± 2.48	0.63	0.85 ± 0.30	2.23 ± 0.75	0.63
Size: $l \times w \times d$ (m)	38 × 14 × 0.6	143 × 18 × 0.9	12 × 9 × 1.5	55 × 18 × 1.5	30 × 15 × 1	40 × 20 × 1	37 × 18 × 1.5	70 × 7 × 1
Hydraulic residence time (h)[g]	26	6	32	35	100	130	64	108
pH	6.54 ± 0.34	6.79 ± 0.60	6.03 ± 1.09	6.08 ± 0.57	4.84 ± 0.27	6.60 ± 0.20	6.14 ± 0.40	4.88 ± 0.19
Mn (mg/L) in	34.7 ± 14.0	9.4 ± 1.4	55.5 ± 37.0	31.2 ± 0.10	150 ± 13.8	19.4 ± 3.1	19.9 ± 7.1	18.4 ± 1.1
Mn (mg/L) out	8.6 ± 10.3	1.7 ± 1.3	30.9 ± 27.0	17.1 ± 7.02	70	1.3 ± 1.5	23.5 ± 6.0	0.29
Fe (mg/L)	0.16	<0.01	<0.01	<0.01	<0.01	<0.01	<0.01	0.27
Al (mg/L)	0.04	0.04	0.25	1.29	8.25	0.06	0.16	2.48
Ca (mg/L)	190	269	343	183	311	285	167	187
Mg (mg/L)	101	117	183	102	387	166	100	177
Na (mg/L)	1.94	10.6	26.2	11.5	42.7	2.17	9.34	17.6
K (mg/L)	0.75	13.8	7.84	17.5	28.4	5.78	15.1	5.91
Si (mg/L)	8.49	4.17	3.46	8.51	5.15	6.16	9.63	3.59
Organic carbon (mg/L)	41.9	0.86	0.96	0.79	2.09	10.1	0.76	12.1
Total nitrogen (mg/L)	1.53	0.92	0.64	1.34	0.33	3.38	0.16	0.72
Phosphorus (mg/L)	0.18	0.08	0.06	0.12	0.11	0.10	0.09	0.09
Alkalinity (mg $CaCO_3$/L)	–	–	59.3 ± 52.8	21.1 ± 17.6	28	68.6 ± 25.5	28.1 ± 17.6	5.0
Dissolved oxygen (mg/L)	1.8	–	2.5 ± 2.4	6.3 ± 1.6	6.2 ± 0.6	6.9	7.6 ± 2.1	3.6
GDM (g Mn(II)/d m^2)	6.9	14	14	7.4	9.7	1.8	-1.0	1.9
GPS coordinates	40°29′12″N, 78°30′51″W	35°33′40″N, 85°26′10″W	41°08′32″N, 79°50′16″W	41°08′40″N, 79°49′55″W	41°2′105″N, 78°39′16″W	40°18′45″N 79°18′25″W	41°08′33″N, 79°49′48″W	40°03′01″N, 78°48′39″W

Values reported as mean or mean ± standard deviation for n measurements.
[a] Values were averaged from 2009 to 2010, n = 5 (03/09, 06/09, 12/09, 04/10, 08/10).
[b] Values were averaged from 2009, n = 26 (01/09–12/09).
[c] Values were averaged from 2009 to 2010 using data from http://www.datashed.org/. De Sale 1, n = 6 (03/09, 06/09 (2), 09/09, 12/09, 04/10); De Sale 2, n = 4 (06/09, 09/09, 12/09, 04/10); De Sale 3, n = 4 (03/09, 06/09, 12/09, 04/10).
[d] Values were averaged from 2005 to 2010, n = 9 (12/05, 04/06, 06/06, 01/07, 06/07, 10/07, 06/09, 11/09, 04/10).
[e] Values were averaged from 2009 to 2010, n = 3 (10/09, 07/10, 08/10).
[f] Values were averaged from 2006 to 2010, n = 5 (02/06, 07/06, 06/07, 10/07, 08/10).
[g] Hydraulic residence times were calculated using the average flow rate and assuming a bed porosity of 0.5 vol/vol (Watzlaf et al., 2004).

the sediment) in 120 mL serum bottles and sealed with thin Teflon-coated stoppers and Al crimp tops. Manganous chloride was added to all reactors such that the initial concentration of dissolved Mn(II) was 170 mg/L (regardless of Mn(II) concentration in site water). "Live" reactors contained air in the headspace. Abiotic controls were prepared with sterilized sediments that been exposed to 100 kilogray of ^{60}Co γ irradiation and maintained under a 100% N_2 headspace (referred to hereafter as "sterile/N_2"). Fungicide-amended reactors were prepared with 0.6 g/L cyclohexamide and 0.6 g/L pentachloronitrobenzene to operationally eliminate the contribution of fungi on Mn removal (referred to hereafter as "live + fungicides"). Additionally, a sediment-free control experiment was run under an air headspace.

All reactors were kept in the dark and shaken at 100 rpm on an orbital shaker at room temperature (22–24 °C). Water and sediment suspension samples were periodically collected from the reactors using a sterile needle and syringe to measure dissolved Mn(II) and pH. Samples were centrifuged at 11,000g for 10 min to separate liquid and sediments. Mn(II) concentrations in the supernatants were measured using the PAN method (Goto et al., 1977). pH was measured using a combination electrode (Thermo Scientific, Waltham, MA). When the soluble Mn(II) concentration decreased to <30 mg/L in the "live" reactors, $MnCl_2$ was re-spiked into all the reactors to re-establish a Mn(II) concentration of approximately 170 mg/L. Manganous chloride was added to the reactors four to eight times depending on the site.

2.3. Rate calculations and operational definitions

A lumped zero-order Mn(II) removal rate (d[Mn(II)]/dt; mg Mn/h g sediment) was calculate over the final four fed-batch cycles (denoted by time period right of vertical dashed line and horizontal arrow in Fig. 2) according to:

$$\mathrm{d[Mn(II)]/dt} = \frac{\sum_{n=1}^{4}([\mathrm{Mn(II)}]_{0,n} - [\mathrm{Mn(II)}]_{\mathrm{f},n}) \times V}{\Delta t_n \times m} \quad (1)$$

where $[Mn(II)]_{0,n}$ and $[Mn(II)]_{f,n}$ are the dissolved Mn(II) concentrations (mg Mn/L) at the start and finish of the nth fed-batch cycle (i.e., number of Mn spike), Δt_n is the duration of the nth fed-batch cycle (h), V is the water volume in the reactor (L), and m is the sediment mass in the reactor (g sediment). The collection of well-mixed suspension samples caused the V/m ratio to remain constant throughout the experiment.

Eq. (1) was used to calculate lumped zero-order Mn(II) removal rates for the "live", "sterile/N_2" and "live + fungicide" reactors. The total Mn(II) removal rates from the "live" sediment reactors were operationally defined (Table 3). Also using Eq. (1), the lumped contribution of *Adsorption + Precipitation* from the "sterile/N_2" reactors was operationally defined. In the absence of a biological catalyst, it was assumed that Mn(II) could be lost from solution via adsorption to the sediments or, at least initially, via precipitation as $MnCO_3(s)$ ($\log K_{sp} = -10.6$). The lumped contribution of O_2-*driven oxidation* was then operationally defined according to:

$$\{\mathrm{d[Mn(II)]/d}t\}_{\mathrm{O2\text{-}driven\ oxidation}} = \{\mathrm{d[Mn(II)]/d}t\}_{\text{"live"}} - \{\mathrm{d[Mn(II)]/d}t\}_{\text{"sterile/N2"}} \quad (2)$$

where the O_2-driven processes include bacteria-, fungi-, and MnO_x-mediated oxidation (Table 3). In a similar manner, the lumped contribution of *Bacterial + Abiotic Oxidation* was operationally defined according to:

$$\{\mathrm{d[Mn(II)]/d}t\}_{\mathrm{Bacterial+Abiotic\ MnOx}} = \{\mathrm{d[Mn(II)]/d}t\}_{\text{"live+fungicide"}} - \{\mathrm{d[Mn(II)]/d}t\}_{\text{"sterile/N2"}} \quad (3)$$

where the fungal contribution was presumably eliminated by the fungicides and the *Adsorption + Precipitation* contributions were presumably the same in both the "live + fungicide" and "sterile/

Fig. 1. Freshly collected sediments from the Mn(II)-removal beds. (A) Ace, (B) Glady Fork, (C) De Sale 2, (D) De Sale 1, (E) De Sale 3, (F) Fairview, (G) Derry Ridge, and (H) PBS. Soil-like sediments in A–D. Sediments with MnO_x crusts in E–H. Ruler scale = cm.

N_2" reactors. Finally, the individual contribution of *Fungal Oxidation* was operationally defined according to:

$$\{d[Mn(II)]/dt\}_{Fungal} = \{d[Mn(II)]/dt\}_{\text{"live"}} - d[Mn(II)]/dt_{\text{"live+fungicide"}} \quad (4)$$

where the *Bacterial + Abiotic Oxidation*, and the *Adsorption + Precipitation* contributions were presumably the same in both the "live" and "live + fungicide" reactors.

Field performance of the Mn(II)-removal beds was based on measurements of the influent flow rate, influent and effluent water chemistry, the dimensions of the bed, and an assumed bed porosity of 50% (vol/vol) (Watzlaf et al., 2000) for all sites. The field-based zero-order Mn(II) removal rate (mg Mn/h m^3 limestone) was calculated according to:

$$\{d[Mn(II)]/dt\}_{field} = \frac{[Mn(II)]_{in} - [Mn(II)]_{out}}{\theta_H \times V_{limestone}} \quad (5)$$

where $[Mn(II)]_{in}$ and $[Mn(II)]_{out}$ are the influent and effluent dissolved Mn(II) concentrations (mg Mn/L), Θ_H is the hydraulic residence time of the water in the Mn(II)-removal bed (h), and $V_{limestone}$ is the volume of limestone in the bed (m^3 limestone). Θ_H was calculated as the bed water volume (i.e., 50% of total bed volume) divided by the influent flow rate.

2.4. Analytical methods

Water samples were analyzed for dissolved metals, total organic C (TOC), total organic N (TN) and total P. Cations (Al, As, Ca, Co, Cr, Cu, Fe, K, Mg, Mn, Na, Ni, Si, Sr, Ti, Zn) were measured using a Perkin–Elmer Optima 5300 inductively coupled plasma atomic emission spectrophotometer (ICP-AES). TOC and TN were measured using a Shimadzu TOC-VCSH analyzer. Total P was measured using the Hach PhosVer 3 Acid Persulfate Digestion Test 'N Tube Method 8190.

Elemental analysis of the sediments was performed by lithium metaborate fusion followed by ICP-AES. Briefly, sediment samples were dehydrated, heated to 750 °C overnight to remove organic matter, mixed with lithium metaborate and heated to 900 °C, and mixed with 5% HNO_3 before analysis. Silica was needed to melt some of the sediments and, therefore, SiO_2 concentrations could not be determined. Elemental sediment concentrations were reported in oxide form based on the dry sediment mass. Sediment

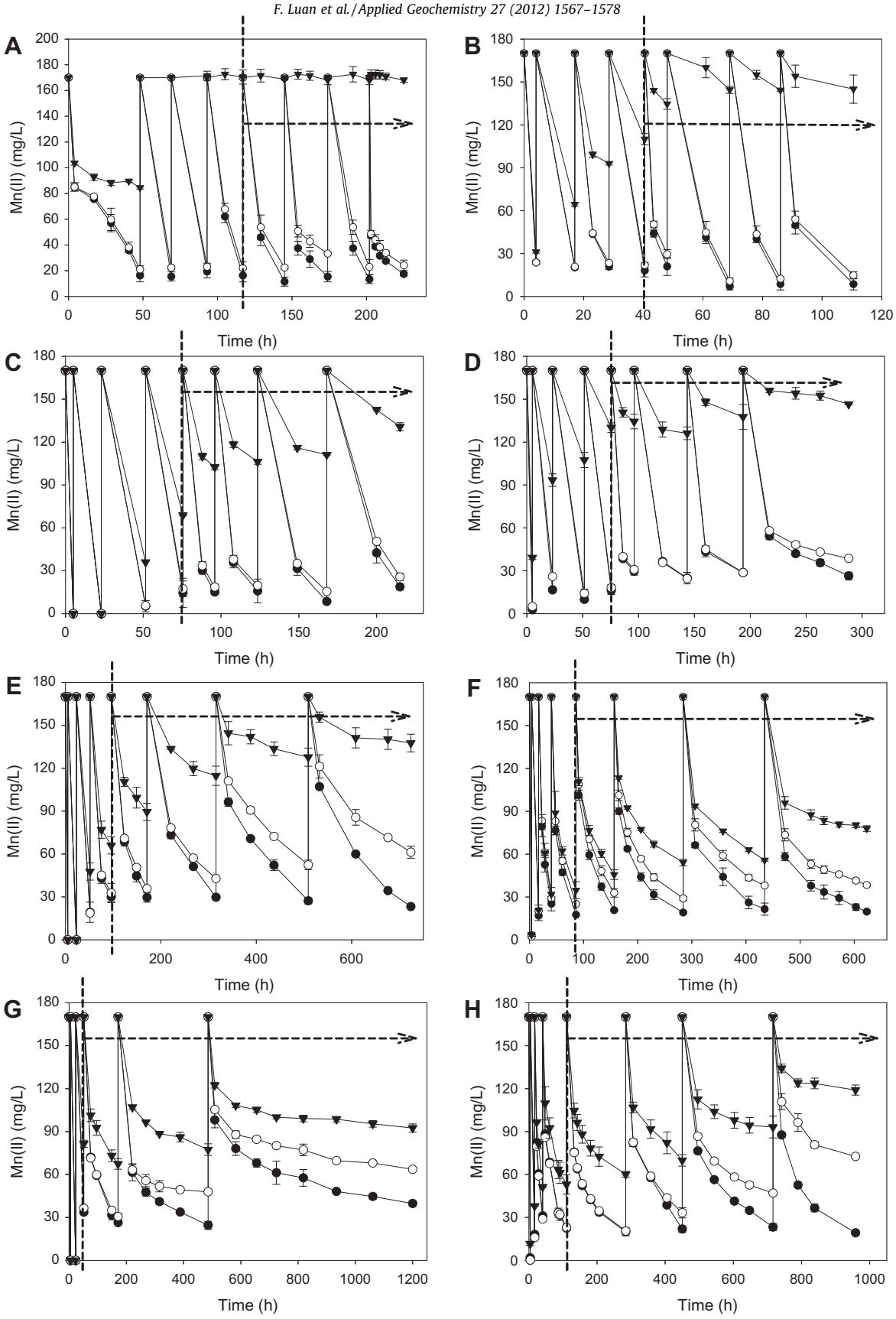

Fig. 2. Mn(II) loss from solution in laboratory sediment incubation experiments. Sediments were divided into "fast" (A–D) and "slow" (E–H) groups based on total Mn(II) removal rate. (A) Ace, (B) Glady Fork, (C) De Sale 3, (D) De Sale 2, (E) Fairview, (F) Derry Ridge, (G) De Sale 1 and (H) PBS. Black circles were "live" reactors; white circles were "live + fungicides" reactors; black triangles were "sterile/N_2" (γ irradiation) reactors. Live reactors were maintained under air while the sterile reactors were maintained under 100% N_2. Mn(II) was repeatedly spiked (as $MnCl_2$) to increase the Mn(II) concentration back to ca. 170 mg/L once it dropped below ca. 30 mg/L in the "live" reactors. Experiments were conducted with 0.50 g MnO (dry) and 50 mL filter sterilized influent site water. Lumped zero-order Mn(II) removal rates were calculated over the final four fed-batch cycles (three for G) according to Eq. (1), which are denoted by the time period right of the dashed vertical line and horizontal arrow.

surface area was measured by N_2 BET using a Micromeritics ASAP 2020 surface area and porosity analyzer.

2.5. Phospholipids fatty acids (PLFA)

Analysis of PLFAs was performed on MnO_x-rich sediments collected from the "live" incubation experiments. Upon completion of the experiments, sediments were frozen at −80 °C to prevent degradation of the fatty acids. Frozen sediments were packed in dry ice and shipped overnight to Microbial Insights, Inc. (Rockford, TN, USA) for lipid extraction and analysis. Briefly, sediments were thawed and lipids were extracted using a one-phase chloroform–methanol-buffer following a modified Bligh and Dyer method (White et al., 1979). Recovered lipids were fractionated into neutral lipids, glycolipids, and polar lipids using disposable silicic acid columns. The polar lipid fraction was transesterified by mild alkali methanolysis to recover the PLFAs as fatty acid methyl esters. PLFAs were determined on a gas chromatograph–mass spectrometer (GC–MS) with electron ionization.

PLFA nomenclature follows the common convention of A:BωC (White et al., 1997). The total number of C atoms in the fatty acid is denoted in position A. Position B is the number of double bonds. Position C designates the position of the C atom from the methyl end (ω) of the molecule before the double bond. *Cis* or *trans* configurations are indicated by 'c' or 't', respectively (Table 5). The prefixes 'i' or 'a' indicate isobranching or anteisobranching, and 'me' indicates the position of the methyl group from the carboxyl-end. Cyclopropyl fatty acids are designated as 'cy'.

This study follows previous recommendations for distinguishing the fungal and bacterial biomass components (Frostegard and Baath, 1996; Bardgett and McAlister, 1999; Baath and Anderson, 2003). Some microbes produce characteristic or specific lipid biomarkers as discussed in those previous methods. For example, the PLFA 18:2ω6 is prominent in fungus (Zelles, 1999; Frostegard and Baath, 1996) and the fatty acids 10me15:0–10me18:0 are primarily found in sulfate reducing bacteria (Zelles, 1997, 1999). In many cases, however, a type of PLFA is present in a wide variety of different organisms. For example, while the PLFA 18:2ω6 was used as an indicator of fungal biomass it is also present in higher eukaryotic organisms such as plants (Olsson et al., 2005). That said, for this study it was appropriate to use 18:2ω6 strictly as a fungal biomarker as it was unlikely that these other eukaryotes were alive in the incubation experiments. It is not possible, however, to discern a fungal or bacterial association for 18:1ω9c, which can sometimes be used as an indicator for fungi (Frostegard et al., 2010). Thus, under these conditions, the PLFA 18:2ω6 was used as a fungal biomass indicator and the following PLFAs were used to determine total bacterial biomass: i14:0, i15:0, a15:0, i16:0, i17:0, a17:0, cy17:0, 18:1ω7c, 18:1ω7t, cyl9:0, 10me16:0, 10me17:0, 10me18:0, 15:0, and 17:0.

3. Results and discussion

3.1. Mn removal

Eight field sites were selected for this study to obtain a broad comparative view of how these different Mn(II)-removal beds performed and to gain a better understanding of the Mn(II)-oxidation processes that influence the success of Mn remediation from CMD. The systems varied with respect to their influent chemistry, flow rate and hydraulic residence time (Table 1). All systems had very low influent concentrations of Fe and Al. While these systems all started with "clean" limestone, over time an abundance of MnO_x precipitates coated the limestone cobbles and/or filled the porous voids in the beds. In collecting MnO_x-rich sediments for the experiments, it was noted that in four of the eight beds (Ace, Glady Fork, De Sale 2, De Sale 1) the sediments accumulated as very thick and soft soil-like material in the porous voids between cobbles that were completely armored by MnO_x coatings (Fig. 1). In contrast, in the other four beds (De Sale 3, Fairview, Derry Ridge, PBS) the sediments accumulated as thin, hard MnO_x coatings (i.e., "crusts") that had to be mechanically scraped from the stones for collection. Solid-phase concentrations of Mn oxides (MnO) varied from 18 to 55 mass% for the materials used in the laboratory experiments with higher concentrations found in the "soil-like" sediments (Table 2). Limestone fragments were also collected with the sediments. Solid-phase concentrations of CaO + MgO varied from 5 to 25 mass% with higher concentrations found in the "crusts" (Table 2).

Reactors containing wet-sieved (<2-mm) MnO_x-rich sediments and their associated natural microbial communities were operated in a fed-batch mode with respect to dissolved Mn(II), i.e., experiments were repeatedly spiked with dissolved Mn(II) for the purpose of distinguishing abiotic processes from oxidative Mn removal. While sediment texture in the field varied from soft soil-type to hard crusts (Fig. 1), the sieved materials used in the laboratory reactors were all relatively similar with respect to particle size and texture (Supp. Fig. S2). Differences in XRD patterns (Supp. Fig. S3) and SEM images (Supp. Fig. S4) from the field sediments were difficult to distinguish. The rate of Mn(II) removal from the laboratory sediment reactors varied considerably with the different sediments (Table 4). Even for a single sediment, the rate of Mn(II) removal varied over the course of the whole fed-batch reaction period (as observed in Fig. 2). Typically Mn(II) was removed very quickly in the first several fed-batch cycles presumably due to precipitation of $MnCO_3$(s) and adsorption and then slowed in the later cycles.

Dissolved alkalinity in these waters ranged from 0.1 to 1.3 mM (as $CaCO_3$) (Table 1) and could have been consumed with the first spike of 170 mg/L Mn(II) (3.1 mM) to form $MnCO_3$(s). Additionally, solid CaO and MgO in the sediments (Table 2) could have provided a reservoir of alkalinity and allowed $MnCO_3$(s) to form in later stages of the experiments. Differing behavior in the sterile/N_2 controls for the various sediments was not likely controlled solely by differences in the alkaline content of the sediments. For example, the sterile/N_2 controls for the Derry Ridge (Fig. 2F) and De Sale 1 (Fig. 2G) sediments continued to remove Mn(II) throughout the experiment yet these two sediments had the highest and lowest solid-phase contents of CaO + MgO, respectively (Table 2). In comparison, the sterile/N_2 controls for the Ace sediments (Fig. 2A) did not remove any additional Mn(II) in later stages of the experiments suggesting that no additional alkalinity was generated to promote the formation of $MnCO_3$(s) and all Mn(II) adsorption sites were fully exhausted. A limited extent of $MnCO_3$(s) precipitation in the Ace sediment incubations is consistent with its low solid-phase content of CaO + MgO (Table 2).

Because of the variation in rates it was chosen to calculate a lumped zero-order Mn(II) removal rate (Eq. (1)) over the final four fed-batch cycles (denoted by time period right of vertical dashed line and horizontal arrow in Fig. 2) where these abiotic processes became less important. The laboratory-based rates estimated from the fed-batch experiments (Eq. (1)) agreed well with field-based estimates of Mn(II) removal rates (Eq. (5)) from seven sites (Fig. 3). The Fairview site was not included in this correlation because the bed was temporarily off-line when sediments were collected for the laboratory experiments. Using this approach, the field-based and laboratory-based rates of Mn(II) removal were well correlated ($R^2 = 0.87$; $p = 0.002$; Fig. 3). The laboratory-based rates of Mn(II) removal were poorly correlated with Mn oxide content ($R^2 = 0.24$; $p = 0.215$) and sediment surface area ($R^2 = 0.001$; $p = 0.929$) (Supp. Fig. S5).

Table 2
Concentrations of major elements in sediments measured by ICP-AES following lithium metaborate fusion. Values are in oxide forms. SiO_2 was required for sample fusion and, therefore, is not reported.

Concentration (%)	Ace	Glady Fork	De Sale 3	De Sale 2	Fairview	Derry Ridge	De Sale 1	PBS
MnO	55.2	29.4	40.9	47.4	27.9	18.0	50.0	20.1
Al_2O_3	0.15	3.75	7.65	5.67	5.80	6.8	6.09	17.7
BaO	0.01	0.03	0.06	0.07	0.01	0.02	0.05	0.04
CaO	4.11	12.3	10.6	5.02	19.1	23.5	4.20	8.38
CoO	0.06	0.06	0.17	0.27	0.18	0.28	0.81	0.33
Cr_2O_3	0.02	0.01	0.01	0.02	0.01	0.01	0.02	0.01
CuO	0.00	0.00	0.00	0.00	0.01	0.02	0.00	0.02
Fe_2O_3	0.71	4.38	3.79	2.02	0.63	0.62	3.90	2.23
K_2O	0.17	0.79	0.27	0.54	0.45	0.31	0.65	1.09
MgO	1.45	3.67	1.17	0.99	2.09	1.52	0.82	3.56
CaO + MgO	5.56	16.0	11.8	6.01	21.2	25.0	5.02	11.9
Na_2O	0.03	0.07	0.04	0.07	0.29	0.06	0.04	0.09
NiO	0.07	0.28	0.20	0.32	0.20	0.30	0.30	0.45
SrO	0.05	0.02	0.02	0.02	0.04	0.04	0.02	0.02
LOI (900 °C)	33.1	20.3	22.7	20.8	26.3	28.4	22.1	22.1
BET surface area (m^2/g)	51	42	52	38	24	28	85	65

Table 3
Summary of operative Mn(II)-removal mechanisms in the different reactor treatments, and operational definitions used to calculate the contribution of individual or lumped removal mechanisms.

	Bacteria-mediated oxidation	Fungi-mediated oxidation	Abiotic oxidation with O_2	Non-oxidative Adsorption	Precipitation of $MnCO_3$(s)	Rate contribution determined by Eq. #
"Live" reactors	Yes	Yes	Yes	Yes	Yes	1
"Live + fungicide" reactors	Yes	No	Yes	Yes	Yes	1
"Sterile/N_2" reactors	No	No	No	Yes	Yes	1
O_2-driven Oxidation = "live" reactors – "sterile/N_2" reactors	Yes	Yes	Yes	No	No	2
Adsorption + precipitation = "sterile/N_2" reactors	No	No	No	Yes	Yes	1
Bacterial + abiotic oxidation = "live + fungicide" reactors – "sterile/N_2" reactors	Yes	No	Yes	No	No	3
Fungal oxidation = "live" reactors – "live + fungicide" reactors	No	Yes	No	No	No	4

Table 4
Summary of operationally defined contributions to the Mn(II) removal rate measured in laboratory experiments, and Mn(II) removal rates calculated based on field performance.

	Ace	Glady Fork	De Sale 3	De Sale 2	Fairview	Derry Ridge	De Sale 1	PBS
Sediment texture	soil-like	soil-like	MnO_x crust	Soil-like	MnO_x crust	MnO_x crust	soil-like	MnO_x crust
Total Mn(II) removal rate (μg/h g sed)[a]	318.0	267.7	174.2	123.2	25.4	20.1	18.3	14.1
Relative rate of Mn(II) removal rates	Fast	Fast	Fast	Fast	Slow	Slow	Slow	Slow
Adsorption + precipitation Mn(II) removal rate (μg/h g sed)[b]	3.9	46.9	64.3	29.2	9.4	15.0	11.9	8.0
O_2-driven oxidation Mn(II) removal rate (μg/h g sed)[c]	314.1	219.8	109.9	94.0	16.0	5.1	6.4	6.1
Bacterial + abiotic oxidation Mn(II) removal rate (μg/h g sed)[d]	291.1	210.5	103.9	91.2	12.3	3.2	4.2	4.0
Fungal oxidation Mn(II) removal rate (μg/h g sed)[e]	23.0	9.3	6.0	2.8	3.7	1.9	2.2	2.1
Field Mn(II) removal rate (mg/h m^3 limestone)[f]	469	639	386	202	403	73	−28	80

[a] Total rate calculated from "live" reactors according to Eq. (1).
[b] Adsorption + precipitation Mn(II) removal rate calculated from "sterile/N_2" reactors according to Eq. (1).
[c] O_2-driven oxidation Mn(II) removal rate calculated as the difference between the "live" and "sterile/N_2" reactors according to Eq. (2).
[d] Bacterial + abiotic oxidation Mn(II) removal rate calculated as the difference between the "live + fungicide" and "sterile/N_2" reactors according to Eq. (3).
[e] Fungal Oxidation Mn(II) removal rate calculated as the difference between the "live" and "live + fungicide" reactors according to Eq. (4).
[f] Field Mn(II) removal rate calculated according to Eq. (5).

3.2. Determination of Mn removal processes

One objective of this study was to determine the relative importance of abiotic versus oxidative processes on the removal of Mn(II) from CMD in the various treatment systems. This objective was approached by identifying the major Mn(II) removal mechanisms and operationally defining when these processes would be operative under different experimental conditions (Table 3; Eq. (2)–(4)). It is proposed that Mn(II) is removed by five dominant processes: (1) bacteria-mediated oxidation, (2) fungi-mediated oxidation, (3) abiotic MnO_x-mediated oxidation, (4) non-oxidative adsorption, and (5) precipitation of $MnCO_3$(s). Sediment-free controls under an air headspace showed no loss of Mn(II) so homogeneous Mn(II) oxidation was not considered. It is assumed that all of the potential processes are operative in the "live" reactors and that the relative contribution of individual or lumped processes can be calculated by differences between results obtained with the "sterile/N_2" and the "live + fungicide" reactors. While it is recog-

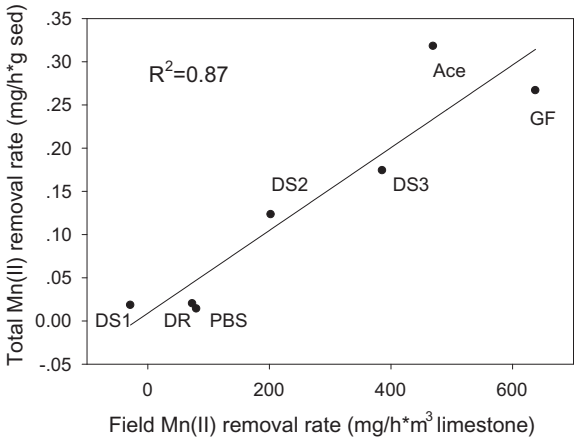

Fig. 3. Correlation between total Mn(II) removal rates measured in laboratory experiments (calculated using Eq. (1)) with Mn(II) removal rates measured in the field (calculated using Eq. (2)). Ace – Ace; DR – Derry Ridge; DS1 – De Sale 1; DS2 – De Sale 2; DS3 – De Sale 3; GF – Glady Fork; PBS – PBS.

nized that this approach is based upon the assumption of superposition of all the operative processes (e.g., abiotic oxidation may become more important in the absence of Mn(II)-oxidizing microbes; bacterial oxidation may become more important in the absence of fungi), the results garnered from all eight sites are valuable on a comparative basis.

In the current study, incubations were not conducted with live sediments under a 100% N_2 headspace (i.e., "live/N_2") to further differentiate the contributions of abiotic oxidation with O_2 versus without O_2. However in previous experiments conducted with live Fairview sediments maintained under a 100% N_2 headspace, very little Mn removal was measured in the latter cycles of Mn(II) addition – results consistent with those obtained with sterile Fairview sediments under air or N_2 headspace (Burgos et al., 2010). Based on these previous results, it is speculated that Mn(II) removal with live or sterile sediments under anoxic conditions would be essentially the same such that *O_2-driven Oxidation* (Eq. (2)) was primarily due to biologically-mediated Mn(II) oxidation.

As seen with the "live" reactors maintained under air versus the sterilized reactors maintained under N_2 (black circles and black triangles, respectively, in Fig. 2), the difference between Mn(II) removal (determined by the disparity in measured Mn(II) concentrations in "live" vs "sterile/N_2" incubations) through each fed-batch cycle increased as the experiment proceeded. In particular, it was found that the rate of Mn(II) removal following each addition of $MnCl_2$ declined after the first few cycles, and that differences between the operational conditions became more apparent as the experiments progressed (Fig. 2). It is presumed that abiotic removal processes became less important and that differences between the operational conditions became more pronounced in the later stages of the experiments. As the experiment progressed, the precipitation of $MnCO_3$(s) became less important as any solid-phase alkalinity would be consumed and reactive sites for Mn(II) sorption would be saturated.

Based on these operational definitions for the kinetic analysis, it was found that the eight field sites could be grouped into two categories of "fast" and "slow" with respect to the total Mn(II) removal rates (rates calculated using Eq. (1); Fig. 4). As noted above, three of the four "fast" sites contained soil-like sediments as compared to MnO_x crusts. For the fast group, with rates ranging from 123 to 318 μg/h g sed, *O_2-driven oxidation* (based on rate contributions in Eq. (3) and dominated by microbial oxidation) accounted for 63–99% of the Mn(II) removal rate (Table 3), while O_2-*driven* oxidation accounted for 25–63% of the Mn(II) removal rate in the slow group (where total Mn(II) removal rates ranged from 14.1 to 25.4 μg/h g sed). *Adsorption + Precipitation* tended to account for more of the Mn(II) removal rate in the slow group (37–75%) as compared to the fast group (1.2–37%). For instance, abiotic Mn(II) removal in the sediments from Derry Ridge, a representative of the "slow" group in Fig. 2F, continued even after seven fed-batch cycles (as seen by decreasing measured Mn(II) concentrations in the sterile/N_2 incubations after the final Mn spike) and exerted a large influence on Mn removal. In contrast, with sediments from Ace (a representative of the "fast" group; Fig. 2A), abiotic Mn(II) removal in these sediments was almost nil after seven fed-batch cycles (i.e., the measured Mn(II) concentrations decreased minimally in the sterile/N_2 reactors after the final Mn spike) and O_2-*driven* oxidation appeared to dominate Mn removal.

3.3. Microbial contributions to oxidative removal

Based on the experimental design and operational definitions the individual contribution of bacteria-mediated oxidation on the Mn(II) removal rate could not be calculated. Instead, the lumped contributions of bacteria-mediated and abiotic oxidation were calculated according to Eq. (3). Based on previous fed-batch experiments with MnO_x-rich sediments (Burgos et al., 2010), it is predicted that the abiotic Mn(II) oxidation by the host Mn oxides is low in comparison to oxidation by bacteria and bacterially-produced MnO_x (noted above). However, since these two processes are intimately linked, teasing out their relative roles is remarkably difficult. That said, the contribution of bacteria-mediated Mn(II) oxidation was much greater in the fast group (91.2–291 μg/h g sed, accounting for 59.8–91.5% of the total rates) as compared to the slow group (4.0–12.3 μg/h g sed, accounting for 15.9–48.4% of the total rates). The contribution of fungi-mediated Mn(II) oxidation was low in all eight soil –like samples, ranging from 2.8 to 23.2 μg/h g sed in the fast group (2.3–7.2% of the total rates) and 1.9–3.7 μg/h g sed in the slow group (9.5–14.9% of the total rates). It should be noted, however, that the decision to agitate the laboratory reactors (100 rpm on an orbital shaker) may have inhibited fungal activity. A quick growth kinetics study of the Mn(II)-oxidizing fungal cultures isolated previously from several of these CMD treatments (Santelli et al., 2010) has since revealed that most of these fungal species cannot grow or grow poorly in agitated growth conditions (data not shown). Thus, these laboratory experiments may not fully reflect the contribution of fungi in the environment.

Interestingly, in previous experiments with Fairview sediments (conducted in the same fed-batch mode and mixed at 100 rpm), it was found that fungal activity accounted for over 80% of Mn removal (Burgos et al., 2010). The previous results were obtained with Fairview sediments collected while the bed was on-line and operational. The current results with Fairview sediments (where fungi accounted for 15% of the Mn(II) removal rate) were obtained with sediments collected while the bed had been off-line for over a month (but still water saturated). These differing results may suggest that the microbial community in any one Mn(II)-removal bed is a dynamic characteristic affected by hydrodynamic conditions and other factors (e.g., nutrient shifts, seasonal changes).

To better understand the biomass contribution and makeup of the microbial community existing in the sediments from the fed-batch incubation experiments, the concentration of a variety of phospholipid fatty acids (PLFAs) were measured. PLFAs are a primary component of both eukaryotic and prokaryotic cell membranes that generally decompose rapidly upon cell death. Because of these characteristics, the quantification of PLFAs in an environment is an effective way to measure the living biomass. The total PLFA concentration was measured at the completion of each "live" fed-batch laboratory experiment in this study. Due to

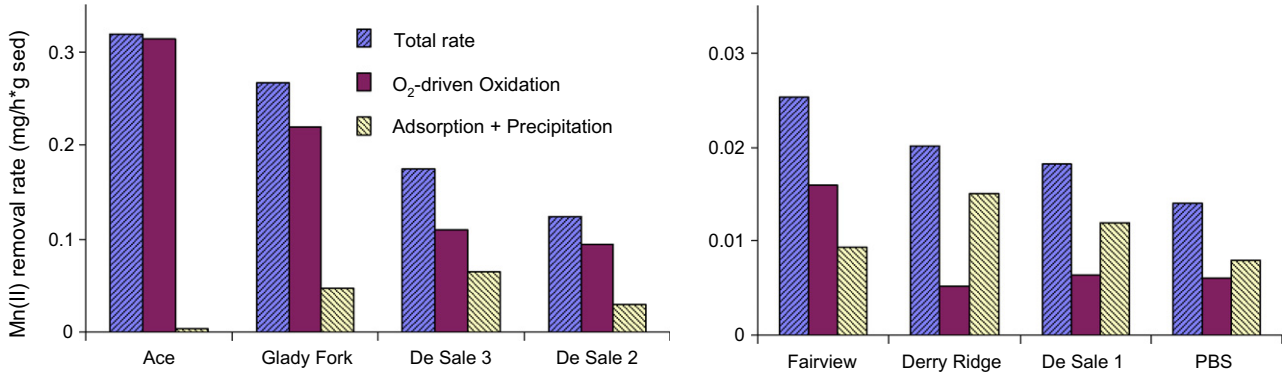

Fig. 4. Relative contributions of O_2-driven oxidation (primarily biotic; calculated using Eq. (3) with "live" reactors) as compared to adsorption + precipitation (abiotic; calculated using Eq. (1) with "sterile/N_2" reactors). Sediments were divided into "fast" (L-hand panel) and "slow" groups (R-hand panel) based on their total Mn(II) removal rate.

the conditions imposed during the experiments (i.e., agitated and dark growth conditions), it is hypothesized that primarily bacteria and non-photosynthetic microeukaryotes can persist and the total PLFA concentration reflects the living microbial biomass. The total measured PLFA (Table 5) ranged from 2960 pmol/g sediment in the Derry Ridge experiments to 108,000 pmol/g sediment in the Ace experiments – a difference of nearly two orders of magnitude in microbial biomass between the field sites. The sites supporting the greatest biomass included Ace, Glady Fork, De Sale 2, and De Sale 1 with >10,000 pmol/g sediment. All other sites (De Sale 3, Fairview, Derry Ridge, and PBS) supported a lower microbial biomass under these experimental conditions.

In addition to microbial biomass, PLFA analysis provides information about the general composition of the microbial community. The measured concentrations for a total of 36 different PLFAs are shown in Table 5 along with their common group associations. It is clear that the total eukaryotic biomass is considerably less than that for the total prokaryotic biomass at the completion of the laboratory experiments (samples collected only from "live" reactors). When using the biomarkers specific to bacteria and fungi (as described in the Materials and Methods section), it is apparent that bacteria are much more prevalent than fungi in these experiments. In particular, the relative fungal:bacterial biomass ratio was <0.4 at the completion of all experiments, and $\leqslant$0.1 for all but the De Sale 2 and De Sale 3 experiments (Table 5). This ratio is only an approximation, as the specificity or group association of a number of the measured biomarkers is not established. The lower fungi:bacteria values for the majority of the experiments are consistent with those measured using similar techniques in a variety of forest soils (Baath and Anderson, 2003).

The only statistically robust correlation between microbial biomass (defined by PLFA) and Mn(II) removal rates was observed between the bacterial biomass and O_2-*driven* oxidation, which was positively correlated ($R^2 = 0.62$; $p = 0.020$) (Fig. 5). A less significant correlation was obtained for total biomass ($R^2 = 0.55$; *$p = 0.035$) and* O_2-*driven* oxidation. The lower correlation, when considering total biomass, was due to the poor correlation between fungal biomass and oxidative removal ($R^2 = 0.10$; correlation not shown) suggesting that the fungi were not dominant contributors to Mn(II) oxidation (possibly due to the experimental setup). Thus, in general, the greater the concentration of bacterial biomass the faster the Mn(II) removal rates provides evidence that the bacterial community is responsible for a substantial proportion of the Mn(II) oxidation in these experiments. DeSale 1 (DS1) was an exception to this trend and, in fact, removing it from the data set resulted in a considerably better correlation between bacterial biomass and oxidative rate ($R^2 = 0.76$). At De Sale 1 the oxidative Mn(II) removal rates were "slow" despite having a high biomass. This may suggest that there was a low relative proportion of Mn(II)-oxidizing microbes in the total bacterial community and thus abiotic processes dominated. In contrast, the bacterial community in the De Sale 3 (DS3) experiments appeared to be dominated by Mn(II)-oxidizers as the "fast" Mn(II) removal rate was supported by a relatively low total biomass. This interpretation is further supported by the data in Fig. 2, which suggest that *Adsorption + Precipitation* dominated in the "slow" incubation (Fig. 2E–H) whereas O_2-*driven* oxidation dominated in the "fast" incubations (Fig. 2A–D).

Even though dramatically different Mn(II) removal rates were observed in the experiments, a plot of the mole percentage of the general types of PLFAs recovered from each "live" Mn removal experiment (Fig. 6) shows that the relative proportion of each class (e.g., monoenic fatty acids or mid-chain branched saturated fatty acids) was similar between all sites. These results suggest that a similar microbial community developed in all the sediments in response to the laboratory growth conditions and that this community had a small proportion of fungal biomass (indicated by the "F" in the polyenoics segment in Fig. 6). The low abundance of fungal biomass and lack of correlation with Mn(II) oxidation suggests that fungal activity was not a dominant pathway for Mn removal in these experiments. No culturing work was performed in this study, however, to specifically identify the Mn(II)-oxidizing microorganisms and, although unlikely, the possibility of low abundance microorganisms contributing appreciably to Mn(II) oxidation rates cannot be ruled out.

3.4. Environmental significance

The removal of Mn(II) from CMD is a costly process. The ability to predict the performance of Mn(II)-removal beds would at least make their design less uncertain. In this study it was demonstrated that a simple fed-batch laboratory experimental protocol was well correlated to field-scale performance of seven Mn(II)-removal beds (Fig. 3). Furthermore, microbial biomass (measured as PLFA) was the only sediment characteristic that correlated with the laboratory-based Mn(II) removal rates. These results support a popular assumption that microbial oxidation of Mn(II) is more significant than abiotic sorption and oxidation. However, it was found that abiotic processes still contributed substantially to Mn removal (37–75%) in five of the eight sediments and the relative contribution of abiotic and biotic processes varied among the sites.

In the case of CMD treatment systems where one starts with a "clean" limestone bed, the relative importance of either biotic or abiotic processes will depend on the age of the bed, the extent of MnO_x precipitates in the bed, and the nutrient status of the influent

Table 5
Concentrations and distributions of phospholipid fatty acids (PLFAs) extracted from the different field sediments collected from the "live" reactors at the conclusion of the laboratory fed-batch experiments.

PLFA (pmol/g sediment)	Ace	Glady Fork	De Sale 3	De Sale 2	Fair-view	Derry Ridge	De Sale 1	PBS	Common group associations[a]
Total measured	107,963	29,446	6234	66,060	9330	2959	35,026	7335	
Bacterial biomass	39,119	12,044	2050	12,647	4324	971	14,375	3055	
Fungal biomass	2396	353	324	4928	147	16	953	75	
Fungi/bacteria	0.06	0.03	0.16	0.39	0.03	0.02	0.07	0.02	
Bacteria									
TerBrSats[b]									*Gram Positives*
i14:0	1176	259	9	165	34	2	91	10	Bacteria*
i15:0	3540	2879	292	2100	552	75	1632	251	Bacteria*
a15:0	1317	1681	84	938	248	42	756	126	Bacteria*
i16:0	1155	445	85	528	216	26	490	81	Bacteria*
i17:0	1176	406	105	641	261	39	630	177	Bacteria*
a17:0	960	303	70	429	179	22	396	108	Bacteria*
Monoenics									*Gram Negatives, Proteobacteria*
15:1ω6c	86	44	0	0	5	0	0	4	
16:1ω9c	1554	633	139	581	175	148	529	249	
16:1ω7c	14,073	4171	484	3309	515	398	2805	448	
16:1ω7t	421	127	15	132	34	20	84	17	
16:1ω5c	5191	1125	204	826	259	41	1716	125	Bacteria, AM fungi
17:1ω8c	227	94	16	145	27	7	123	16	
17:1ω6c	173	209	16	132	54	7	98	106	
cy17:0	3356	1163	214	786	405	162	1520	318	Bacteria*
18:1ω9c	8051	1334	860	7722	494	75	1677	281	Gram positives, Fungi, Plants
18:1ω7c	18,681	2352	570	3190	896	259	3765	714	Bacteria*, AM fungi
18:1ω7t	550	68	18	112	67	15	144	29	Bacteria*
18:1ω5c	1856	427	32	165	35	0	210	32	
19:1ω6c	0	0	8	0	23	11	0	15	
cy19:0	4533	1013	342	1783	584	155	2598	529	Bacteria*
BrMonos[c]									*Anaerobes, Microaerophiles*
i17:1ω7c	421	277	115	343	204	29	508	212	
br19:1a	3443	274	133	799	167	56	648	101	
MidBrSats[d]									*Sulfate reducers, Gram Positives*
10me16:0	755	889	134	647	505	88	1355	467	Bacteria*
12me16:0	151	38	26	92	38	14	56	12	
10me17:0	237	138	20	139	77	15	221	51	Bacteria*
10me18:0	259	68	42	238	134	37	329	117	Bacteria*
Eukaryotes									
Polyenoics									
18:2ω6	2396	353	324	4928	147	16	953	75	Fungi*
18:3ω3	626	130	44	1658	27	0	151	10	Algae, Fungi, Plants
20:4ω6	453	156	75	3970	42	0	438	0	Algae, Protists,
20:5ω3	324	144	35	1143	0	0	137	0	Algae
All Organisms									
NormSats[e]									
14:0	1209	639	75	7213	93	12	392	49	
15:0	712	212	27	568	73	15	196	32	Bacteria*
16:0	24,347	5249	1295	16,903	1928	800	6429	1360	
17:0	712	168	38	383	93	19	252	45	Bacteria*
18:0	3572	1884	264	3118	680	340	3537	1113	
20:0	270	97	23	231	56	17	161	52	

[a] The group associations for the different PLFAs are not definitive but are generalizations. Italicized groups refer to the general class of fatty acids whereas roman font groups refer to a specific fatty acid.
[b] Terminally branched saturated (TerBrSats) fatty acids.
[c] Branched monoenic fatty acids.
[d] Mid-chain branched saturated (MidBrSats) fatty acids.
[e] Normal saturated (NormSats) fatty acids.
* Biomarker used to calculate either total bacterial or total fungal biomass.

water to support microbial growth, and will thus vary over the operational lifetime of the bed. Furthermore, the composition and distribution of the dominant Mn(II)-oxidizing microorganisms (and their relative rates of oxidation *in situ)* as well as the relationships (symbiotic or not) and interactions of these organisms with the entire microbial community may be an important factor in the success of these treatment beds. These factors are largely unknown at present and require future investigations. In any case, these studies indicate that the presence of microbial biomass and MnO_x precipitates will enhance Mn removal performance. Therefore, the "seeding" of new Mn(II)-removal beds with MnO_x-coated limestone and associated biomass (collected from older, operational beds and placed near the influent end of the new bed) may be a practical approach to building these beds in the future. This "seeding" should decrease any lag time in establishing a Mn(II)-oxidizing microbial community and allow abiotic MnO_x-catalyzed Mn(II) oxidation to proceed immediately. Combined, these processes should produce more Mn(II)-oxidizing microbes and MnO_x coatings throughout the bed that, in turn, lead to even greater Mn removal.

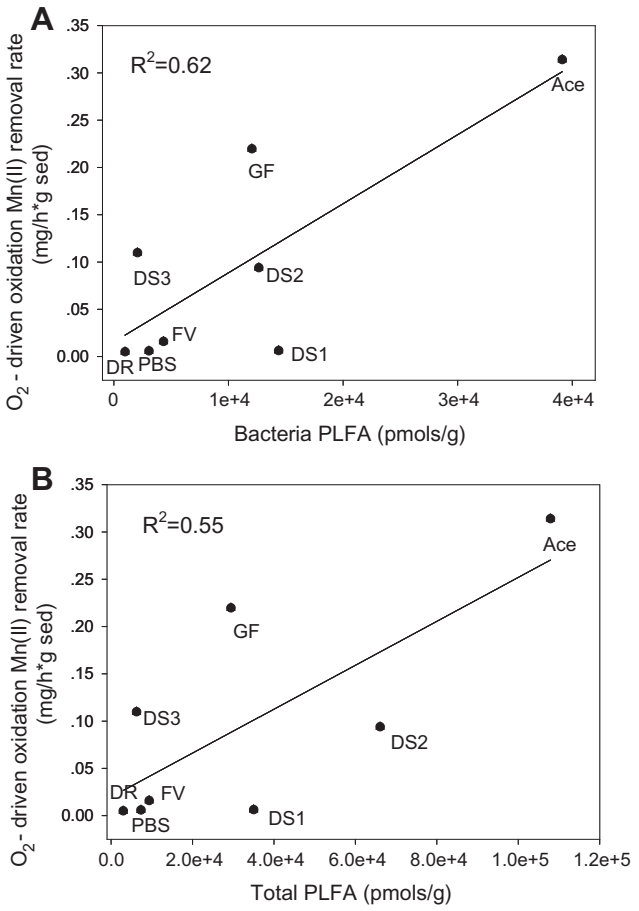

Fig. 5. Correlation of PLFA and O_2-driven Mn(II) removal rate. (A) Content of bacterial PLFA and O_2-driven Mn(II) removal rate. (B) Content of total PLFA and O_2-driven Mn(II) removal rate. PLFAs used to determine bacterial biomass are listed in the Materials and Methods section. Ace – Ace; DR – Derry Ridge; DS1 – De Sale 1; DS2 – De Sale 2; DS3 – De Sale 3; GF – Glady Fork; PBS – PBS.

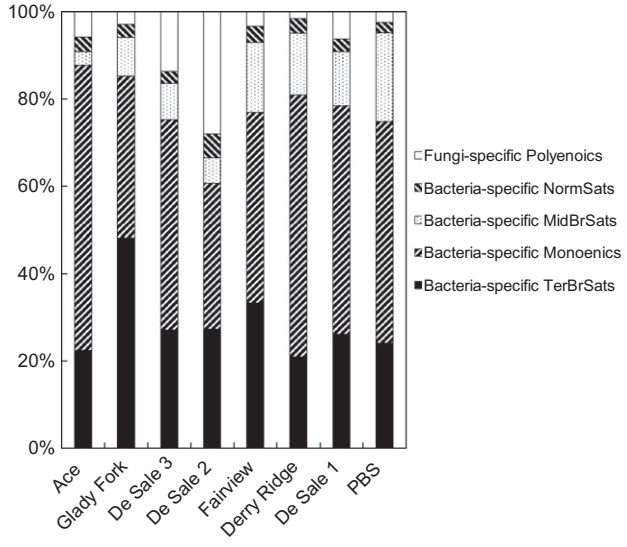

Fig. 6. The mole percentage of fungi- and bacteria-specific PLFAs extracted upon completion of the "live" sediment experiments. The specific biomarkers used for the calculations of each PLFA group are listed in the Materials and Methods section and denoted by asterisks in Table 5. Total PLFA measured for each site (pmol/g) were Ace – 107,963, Glady Fork – 29,446, De Sale 3 – 6234, De Sale 2 – 66,060, Fairview – 9330, Derry Ridge – 2959, De Sale 1 – 35,026, and PBS – 7335.

Acknowledgements

This research was supported by the Office of Surface Mining under Cooperative Agreement S07AP12478 and funds provided by the National Science Foundation, Grant Number EAR-0846715, awarded to CMH.

Appendix A. Supplementary material

Supplementary data associated with this article can be found, in the online version, at http://dx.doi.org/10.1016/j.apgeochem.2012.03.010.

References

Baath, E., Anderson, T.H., 2003. Comparison of soil fungal/bacterial ratios in a pH gradient using physiological and PLFA-based techniques. Soil Biol. Biochem. 35, 955–963.

Bamforth, S.M., Manning, D.A.C., Singleton, I., Younger, P.L., Johnson, K.L., 2006. Manganese removal from mine waters – investigating the occurrence and importance of manganese carbonates. Appl. Geochem. 21, 1274–1287.

Bardgett, R.D., McAlister, E., 1999. The measurement of soil fungal: bacterial biomass ratios as an indicator of ecosystem self-regulation in temperate meadow grasslands. Biol. Fert. Soils 29, 282–290.

Bargar, J.R., Tebo, B.M., Bergmann, U., Webb, S.M., Glatzel, P., Chiu, V.Q., Villalobos, M., 2005. Biotic and abiotic products of Mn(II) oxidation by spores of the marine Bacillus sp. strain SG-1. Am. Mineral. 90, 143–154.

Burgos, W.D., Tan, H., Santelli, C., Hansel, C., 2010. Importance of Fungi in Biological Mn(II) Oxidation in Limestone Treatment Beds, 2010. National Meeting of the American Society of Mining and Reclamation. ASMR, Pittsburgh.

Cravotta, C.A., 2008. Dissolved metals and associated constituents in abandoned coal-mine discharges, Pennsylvania, USA. Part 1: constituent quantities and correlations. Appl. Geochem. 23, 166–202.

Cravotta III, C.A., Trahan, M.K., 1999. Limestone drains to increase pH and remove dissolved metals from acidic mine drainage. Appl. Geochem. 14, 581–606.

Delatorre, M.A., Gomezalarcon, G., 1994. Manganese and iron oxidation by fungi isolated from building stone. Microbial. Ecol. 27, 177–188.

Elzinga, E.J., 2011. Reductive transformation of birnessite by aqueous Mn(II). Environ. Sci. Technol. 45, 6366–6372.

Francis, C.A., Co, E.M., Tebo, B.M., 2001. Enzymatic manganese(II) oxidation by a marine alpha-proteobacterium. Appl. Environ. Microbiol. 67, 4024–4029.

Frostegard, A., Baath, E., 1996. The use of phospholipid fatty acid analysis to estimate bacterial and fungal biomass in soil. Biol. Fert. Soils 22, 59–65.

Frostegard, A., Tunlid, A., Baath, E., 2010. Use and misuse of PLFA measurements in soils. Soil Biol. Biochem. 43, 1621–1625.

Goto, K., Taguchi, S., Fukue, Y., Ohta, K., Watanabe, H., 1977. Spectrophotometric determination of manganese with 1-(2-pyridylazo)-2-naphthol and a nonionic surfactant. Talanta 24, 752–753.

Grote, G., Krumbein, W.E., 1992. Microbial precipitation of manganese by bacteria and fungi from desert rock and rock varnish. Geomicrobiol. J. 10, 49–57.

Haack, E.A., Warren, L.A., 2003. Biofilm hydrous manganese oxyhydroxides and metal dynamics in acid rock drainage. Environ. Sci. Technol. 37, 4138–4147.

Hallberg, K.B., Johnson, D.B., 2005. Biological manganese removal from acid mine drainage in constructed wetlands and prototype bioreactors. Sci. Total Environ. 338, 115–124.

Hansard, S.P., Easter, H.D., Voelker, B.M., 2011. Rapid reaction of nanomolar Mn(II) with superoxide radical in seawater and simulated freshwater. Environ. Sci. Technol. 45, 2811–2817.

Hansel, C.M., Francis, C.A., 2006. Coupled photochemical and enzymatic Mn(II) oxidation pathways of a planktonic Roseobacter-like bacterium. Appl. Environ. Microbiol. 72, 3543–3549.

Herlihy, A.T., Kaufmann, P.R., Mitch, M.E., Brown, D.D., 1990. Regional estimates of acid-mine drainage impact on streams in the mid-Atlantic and southeastern United-States. Water Air Soil Pollut. 50, 91–107.

Johnson, K.L., Younger, P.L., 2005. Rapid manganese removal from mine waters using an aerated packed-bed bioreactor. J. Environ. Qual. 34, 987–993.

Johnson, K.L., Baker, A., Manning, D.A.C., 2005. Passive treatment of Mn-rich mine water: using fluorescence to observe microbiological activity. Geomicrobiol. J. 22, 141–149.

Krumbein, W.E., Jens, K., 1981. Biogenic rock varnishes of the negev desert (Israel) an ecological study of iron and manganese transformation by cyanobacteria and fungi. Oecologia 50, 25–38.

Learman, D.R., Wankel, S.D., Webb, S.M., Martinez, N., Madden, A.S., Hansel, C.M., 2011. Coupled biotic–abiotic Mn(II) oxidation pathway mediates the formation and structural evolution of biogenic Mn oxides. Geochim. Cosmochim. Acta 75, 6048–6063.

Madden, A.S., Hochella, M.F., 2005. A test of geochemical reactivity as a function of mineral size: manganese oxidation promoted by hematite nanoparticles. Geochim. Cosmochim. Acta 69, 389–398.

Mariner, R., Johnson, D.B., Hallberg, K.B., 2008. Characterisation of an attenuation system for the remediation of Mn(II) contaminated waters. Hydrometallurgy 94, 100–104.

Miyata, N., Maruo, K., Tani, Y., Tsuno, H., Seyama, H., Soma, M., Iwahori, K., 2006. Production of biogenic manganese oxides by anamorphic ascomycete fungi isolated from streambed pebbles. Geomicrobiol. J. 23, 63–73.

Miyata, N., Tani, Y., Iwahori, K., Soma, M., 2004. Enzymatic formation of manganese oxides by an Acremonium-like hyphomycete fungus, strain KR21-2. FEMS Microbiol. Ecol. 47, 101–109.

Nealson, K.H., Tebo, B.M., Rosson, R.A., 1988. Occurrence and mechanisms of microbial oxidation of manganese. Adv. Appl. Microbiol. 33, 279–318.

Olsson, P.A., van Aarle, I.M., Gavito, M.E., Bengtson, P., Bengtsson, G., 2005. (13)C incorporation into signature fatty acids as an assay for carbon allocation in arbuscular mycorrhiza. Appl. Environ. Microbiol. 71, 2592–2599.

Pedler, J.F., Webb, M.J., Buchhorn, S.C., Graham, R.D., 1996. Manganese-oxidizing ability of isolates of the take-all fungus is correlated with virulence. Biol. Fert. Soils 22, 272–278.

Ridge, J.P., Lin, M., Larsen, E.I., Fegan, M., McEwan, A.G., Sly, L.I., 2007. A multicopper oxidase is essential for manganese oxidation and laccase-like activity in Pedomicrobium sp ACM 3067. Environ. Microbiol. 9, 944–953.

Robbins, E.I., D'Agostino, J.P., Ostwald, J., Fanning, D.S., Carter, V., Van Hoven, R.L., 1992. Manganese nodules and microbial oxidation of manganese in the Huntley Meadows wetland, Virginia, USA. In: Skinner, H.C. W., Fitzpatrick, R.W. (Eds.), Biomineralization Processes of Iron and Manganese – Modern and Ancient Environments. Catena Supp. 21, pp. 179–202.

Robbins, E.I., Cravotta, C.A., III, Savela, C.E., Nord, G.L., Jr., Balciauskas, K.A., Belkin, H.E., 1997. Hydrobiogeochemical interactions on calcite and gypsum in "anoxic" limestone drains in West Virginia and Pennsylvania. In: 1997 International Ash Utilization Symposium. Univ. Kentucky, Lexington, Ky., pp. 546–559. <http://energy.er.usgs.gov/products/papers/iaus_97/>.

Santelli, C.M., Pfister, D.H., Lazarus, D., Sun, L., Burgos, W.D., Hansel, C.M., 2010. Promotion of Mn(II) oxidation and remediation of coal mine drainage in passive treatment systems by diverse fungal and bacterial communities. Appl. Environ. Microbiol. 76, 4871–4875.

Santelli, C.M., Webb, S.M., Dohnalkova, A.C., Hansel, C.M., 2011. Diversity of Mn oxides produced by Mn(II)-oxidizing fungi. Geochim. Cosmochim. Acta 75, 2762–2776.

Shao, Z.Z., Sun, F.Q., 2007. Intracellular sequestration of manganese and phosphorus in a metal-resistant fungus Cladosporium cladosporioides from deep-sea sediment. Extremophiles 11, 435–443.

Takano, K., Itoh, Y., Ogino, T., Kurosawa, K., Sasaki, K., 2006. Phylogenetic analysis of manganese-oxidizing fungi isolated from manganese-rich aquatic environments in Hokkaido, Japan. Limnology 7, 219–223.

Tan, H., Zhang, G.X., Heaney, P.J., Webb, S.M., Burgos, W.D., 2010. Characterization of manganese oxide precipitates from Appalachian coal mine drainage treatment systems. Appl. Geochem. 25, 389–399.

Tebo, B.M., Bargar, J.R., Clement, B.G., Dick, G.J., Murray, K.J., Parker, D., Verity, R., Webb, S.M., 2004. Biogenic manganese oxides: properties and mechanisms of formation. Ann. Rev. Earth Planet. Sci. 32, 287–328.

Vail, W., Riley, R., 2000. The pyrolusite process: a bioremediation process for the abatement of acid mine drainage. Green Lands 30, 40–46.

Von Langen, P.J., Johnson, K.S., Coale, K.H., Elrod, V.A., 1997. Oxidation kinetics of manganese (II) in seawater at nanomolar concentrations. Geochim. Cosmochim. Acta 61, 4945–4954.

Watzlaf, G., Schroeder, K., Kairies, C., 2000. Long-term performance of anoxic limestone drains. Mine Water Environ. 19, 98–110.

Watzlaf, G.R., Schroeder, K.T., Kleinmann, R.L.P., Kairies, C.L., Nairn, R.W., 2004. The Passive Treatment of Coal Mine Drainage. DOE/NETL-2004/1202, U.S. Department of Energy, National Energy Technology Laboratory, Pittsburgh, PA.

Webb, S.M., Dick, G.J., Bargar, J.R., Tebo, B.M., 2005a. Evidence for the presence of Mn(III) intermediates in the bacterial oxidation of Mn(II). Proc. Natl. Acad. Sci. USA 102, 5558–5563.

Webb, S.M., Tebo, B.M., Bargat, J.R., 2005b. Structural characterization of biogenic Mn oxides produced in seawater by the marine bacillus sp strain SG-1. Am. Mineral. 90, 1342–1357.

White, D.C., Pinkart, H.C., Ringelberg, D.B., 1997. Biomass measurements: biochemical approaches. In: Hurst, C.J., Knudsen, G.R., McInerney, M.J., Stetzenbach, L.D., Walter, M.V. (Eds.), Manual of Environmental Microbiology. ASM Press, Washington.

White, D.C., Davis, W.M., Nickels, J.S., King, J.D., Bobbie, R.J., 1979. Determination of the sedimentary microbial biomass by extractable lipid phosphate. Oecologia 40, 51–62.

Zelles, L., 1997. Phospholipid fatty acid profiles in selected members of soil microbial communities. Chemosphere 35, 275–294.

Zelles, L., 1999. Fatty acid patterns of phospholipids and lipopolysaccharides in the characterisation of microbial communities in soil: a review. Biol. Fert. Soils 29, 111–129.